CALIBRATION AND OPTIMIZATION OF DISCRETE ELEMENT PARAMETERS FOR TIGER NUTS

/

油莎豆种子离散元素参数的标定与优化

Yangyang SHI, Xuejun ZHANG, Jinshan YAN*), Xu MA, Huazhi LI, Changjie HAN
College of Mechanical and Electrical Engineering, Xinjiang Agricultural University, Urumqi 830052, China
Tel: +8615894618255; E-mail: jshan.yan@xjau.edu.cn
Corresponding author: Jinshan Yan
DOI: https://doi.org/10.35633/inmateh-76-84

Keywords: *tiger nuts; contact parameter; Plackett-Burman test; discrete element; simulation*
[1]

ABSTRACT

To improve the accuracy of discrete element simulation parameters for tiger nuts, this study suggests the measurement of the triaxial dimensions of tiger nuts using MATLAB. This method exhibited a maximum error of no more than 0.16% compared to the traditional measurement techniques. Experimental measurements were used to obtain the basic physical parameters of the seeds. Physical tests on the angle of stacking of tiger nuts were conducted. A discrete element model for tiger nuts was constructed. The Plackett-Burman test and the steepest climb test were used to identify critical parameters affecting the angle of accretion and to delineate the optimal range of parameters impacting larger parameters proportionately. The optimum values for the coefficient of static and rolling friction between tiger nuts were established at 0.32 and 0.24, respectively, using response surface methodology. The average tangent of the simulated stacking angle obtained was 0.731 from three tests that carried out using the optimized parameters, representing a mere 0.41% deviation from the physical test average of 0.734. The experimental outcomes confirm that these parameters can provide reliable data for discrete element simulation experiments involving tiger nuts.

摘要

为提高油莎豆种子离散元模拟参数的准确性，本研究提出使用 MATLAB 测量油莎豆种子的三轴尺寸。事实证明，与传统测量技术相比，该方法的最大误差不超过 0.16%。试验测量用于获得种子的基本物理参数。对油莎豆种子的堆积角进行了物理测试。构建了油莎豆种子的离散元模型。利用 Plackett-Burman 试验和最陡爬坡试验确定了影响堆积角的关键参数，并划定了影响较大参数比例的最佳参数范围。利用响应面方法确定了油莎豆种子间静摩擦系数和滚动摩擦系数的最佳值，分别为 0.32 和 0.24。在使用优化参数进行的三次试验中，模拟堆积角的平均正切值为 0.731，与物理试验的平均值 0.734 相比，偏差仅为 0.41%。试验结果证实，这些参数可为有关油莎豆种子的离散元模拟试验提供可靠数据。

INTRODUCTION

Tiger nut, a crop notable for its substantial oil content, is endowed with considerable nutritional value and exhibits a robust adaptability to arid and sandy areas (*Guo et al., 2021*). In recent years, there has been a growing demand for edible oil in China, and the tiger nut, with its uniquely high oil yield, has strategically aligned with national needs. Additionally, its large cultivable area and high harvest rate offer a promising foundation for extensive research (*Li et al., 2022*).

The mechanized sowing of tiger nuts using precision planters introduces intricate interactions among the seeds themselves, and between the seeds and the planter. The constrained dimensions within the seed dispenser render the analysis of these dynamics challenging, necessitating an operational investigation encompassing seed filling, clearing, transporting, and dissemination processes (*Peng et al., 2022; Zhang et al., 2023*). During the seeding process, particles exhibit distinct motion traits individually, along with characteristics of continuous fluid motion, demonstrating pronounced bulk particle dynamics (*Tsa et al., 2021*). The discrete element method is the leading technique for studying the motion of bulk particles, enabling effective simulation of their dynamics and force interactions.

[1] *Yangyang Shi, M.S. Stud.; Xuejun Zhang, Prof. Ph.D.; Jinshan Yan, Prof. Ph.D.; Xu Ma, Prof. Ph.D.; Huazhi Li, M.S. Stud.*

It is widely used in the design of specialized seeders. Due to the irregular surface texture of the tiger nut, both in shape and material properties, it is unsuitable for conventional seeding techniques. To devise a seeder tailored for tiger nuts, an initial investigation into the material properties of these nuts is essential to refine the structural parameters of the specialized seeder, thereby enhancing sowing precision (*Zhang et al., 2021; Xu et al., 2020*).

In seed characterization studies, employing the discrete element EDEM simulation necessitates calibration of several critical parameters, such as inter-particle friction, friction between particles and surfaces, and restitution coefficients (*Chen et al., 2012; Chen et al., 2017; Zhou et al., 2018; Hou et al., 2020*). Some researchers have developed a mung bean model using the bonding model approach, calibrating contact parameters in EDEM simulations to minimizing discrepancies between simulation results and physical testing, thereby refining parameter accuracy (*Zhang et al., 2022*). Some researchers have employed reverse engineering techniques to create discrete element models for cotton seeds, calibrating the contact parameters and aligning the discrepancies in the angle of repose between physical and simulation tests, thereby optimizing the parameters and improve the simulation accuracy (*Wang et al., 2022*). Some researchers have used a rotating drum apparatus to ascertain the contact parameters and angles of repose for cotton seeds, employed these contact parameters as indicators for the mathematical model, and solved the multifactorial optimization through response surface methodology, which proved the reliability and consistency of the discrete element simulation method combined with physical test method (*Hu et al., 2022; Zeng et al., 2021*).

To augment the precision of meta-parameters for tiger nuts, this study proposes integrating theoretical analysis with experimental measurements to derive the seeds' geometrical characteristics, contact parameters and physical properties. Physical and simulation tests were conducted on tiger nuts . Using the Plackett-Burman design, parameters significantly impacting the stacking angle - considered a key evaluation index - were identified. Hill-climbing tests were employed to fine-tune the experimental parameters and obtain the best combination of important parameters, similar to the real-world conditions, for experimental validation. This research provides theoretical references for the study of precision sowing of tiger nuts and the structural parameters of the seeder.

MATERIAL AND METHODS

Rapid calculation of triaxial dimensions of tiger nuts based on image detection

Currently, vernier gauges are predominantly utilized to measure the three-axis dimensions of seeds (*Peng et al., 2022*), a method characterized by low-precision, high labor cost and time-consuming nature. In this study, a MATLAB-based image processing technique is used to ascertain the three-axis dimensions (length L, width W, and thickness T) of tiger nutss, providing sufficient data for EDEM simulation, as illustrated in Fig. 1. Predominantly, tiger nuts exhibit an oval geometry with elongated or abbreviated semiaxes, but also instances of round or irregularly shaped beans occur in random samples. Seeds were sourced from Jiyoudou 21 (JYD-21), a cultivar native to the southern periphery of the Xinjiang Uygur Autonomous Region, China. Considering the practicality and in order to enhance germination efficacy, seeds randomly selected for testing underwent a hydration process, immersing them in water for 4 days before sowing (*Zheng et al., 2024*).

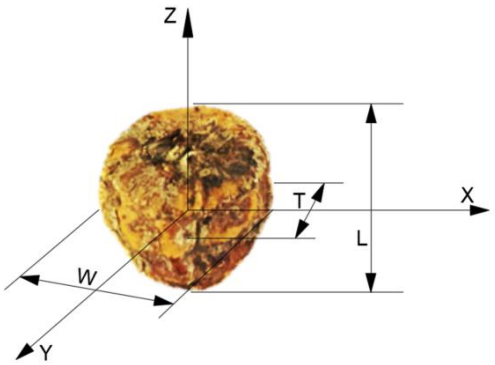

Fig.1 - Schematic diagram of tiger nut characteristic size

Note: L, W, and T are the length, width and thickness of tiger nuts particles)

Seeds were positioned on a shooting plane, photographed by a high-definition industrial camera, and uploaded to a computer (Lenovo R7000p_3050ti) for further analysis with MATLAB. Some of the functions used are not included in the MATLAB library but are still applicable. First of all, the use of function imread was deployed to import the image, as depicted in Fig. 2 (a). Subsequently, the rgb2gray function was applied for grey scale processing, as shown in Fig. 2 (b). The function im2bw was then applied to binarize image processing, as seen in Fig. 2 (c). Owing to significant noise inherent in the image due to capture conditions, a two-dimensional median filtering function medfilt was utilized to denoise the image, as demonstrated in Fig. 2 (d). Considering only the peripheries of the tiger nuts, the use of fill function imfill on the image of the structural elements of the expansion of the processing, as illustrated in Fig. 2 (e). Finally, the use of the regionprops function of the image was calibrated, with the boundaries marked by the red box, as shown in Fig. 2 (f). The centroid, width and length of the depicted tiger nuts were analyzed using the MajorAxisLength and MinorAxisLength functions. The image was scaled in pixel units, with the pixel scale calibrated to a 1 mm unit ratio using the getpois function, which in turn gave the length (mm) and width (mm) dimensions of the tiger nuts. To ascertain the thickness, seeds were positioned on a flat surface in the direction of the thickness and measured in the same way as above.

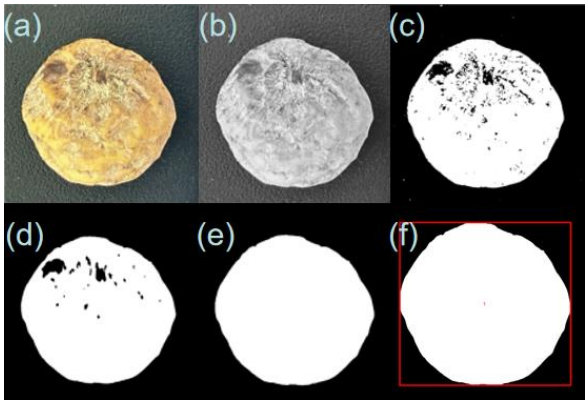

Fig. 2 - Seed image calibration process

In the extant body of research concerning the triaxial dimensional analysis of seeds, vernier gauges are predominantly employed, with no alternative measurement methodologies reported. In order to ascertain the reliability of the data, 60 tiger nuts were randomly selected from a sample of 100 for analysis. The resultant measurements were averaged and contrasted with those typically recorded using vernier gauges, as detailed in existing literature. In this study, compared with the vernier gauge (German SYNTEK digital vernier gauge, accuracy of 0.01 mm), as depicted in Table 1, the measurement errors of the three-axis dimensions (length L (mm), width W (mm), and thickness T (mm) are 0.16 mm, 0.06 mm, and 0.13 mm, respectively, averaging 0.12 mm. In tiger nuts, given the minimal variation in measurement positioning, the occurrence of small discrepancies is expected, however, the rapidity and appropriateness of this method align with the measurement requirements of this paper.

Table 1

Comparison of three-axis dimensional measurements of tiger nuts

Parametric	Length L (mm)	Breadth W (mm)	Thickness T (mm)
Image Inspection/Vernier Calipers	13.07/13.00	12.38/12.33	8.48/8.45
	14.77/14.73	13.67/13.61	7.24/7.16
	14.39/14.11	12.66/12.66	9.28/9.22
	14.46/14.00	13.22/13.02	7.12/7.10
	12.88/12.88	12.17/12.15	8.12/8.02
	13.04/13.02	12.63/12.52	10.11/10.04
Average error in length, width and thickness	0.16	0.06	0.13

Basic physical parameters of tiger nuts

For this study, two hundred seeds were randomly selected and analyzed. Each seed was photographed, and its three-axis dimensions - length (L), width (W), and thickness (T) - were measured. As shown in Table 2, the average values were 12.43 mm, 11.68 mm, and 9.14 mm, respectively, with standard deviations of 1.52 mm, 1.33 mm, and 1.01 mm.

The distribution of these dimensions, illustrated in Fig. 3, follows a bell-shaped curve, i.e., most values are concentrated near the mean, with a gradual decrease and convergence as the values move away from the mean - indicating a normal distribution.

Equation 1 demonstrates that when the size of the three axes is larger, the sphericity is higher, the volume is larger, and the mobility is greater; consequently, the collision force generated by the collision will also increase. Therefore, the selection of materials for seeders needs to be considered to avoid causing significant collision damage to the seeds.

Table 2

Tiger nuts triaxial dimensions

Parametric	Length L (mm)	Breadth W (mm)	Thickness T (mm)
maximum value	15.21	14.11	12.32
minimum value	9.97	8.91	7.01
average value	12.43	11.68	9.14
standard deviation	1.51	1.33	1.01

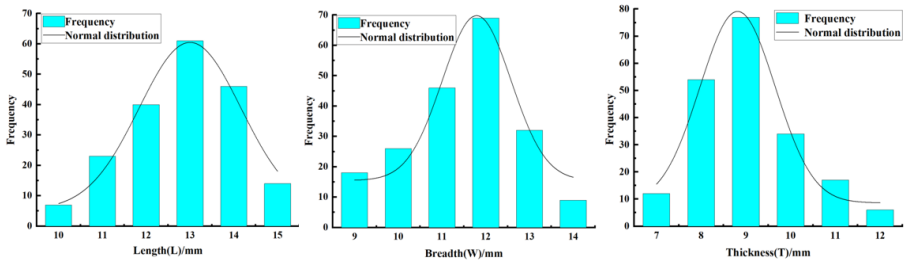

Fig. 3 - Normal distribution of triaxial dimensions of tiger nuts

The volume V, equivalent grain size d, and sphericity S_p of tiger nuts were calculated, with sphericity approaching 100% indicating fuller seeds that more closely approximate a spherical shape (*Chen et al., 2023; Ma et al., 2015*). Repeated 20 times, the mean values of tiger nuts volume V, equivalent particle size d and sphericity S were 1.54 cm^3, 11.15 mm and 85%, respectively, with corresponding standard deviations of 0.12 cm^3, 0.71 mm and 0.97% as listed in Table 3.

The weighing method was used to randomly measure 10 tiger nuts using an MTB1000D-B high precision electronic balance (minimum reading accuracy of 0.01 g). Using a 350 ml beaker, 10 seeds were placed in sequence after the addition of 200 ml of water, ensuring that no air bubbles were present when recording the results of the rise in water level. This process was repeated 10 times, and the average density of tiger nuts was determined to be 1062.22 kg/m^3 (*Chen et al., 2023*). This value is similar to those reported in the relevant literature and is used in this paper to set the structural parameters for subsequent simulations.

A high-precision electronic balance scale (accuracy 0.01 g) was employed to determine the thousand-seed weight, which averaged 789.32 g after 10 repetitions, as shown in Table 3.

$$\begin{cases} V = LWT \\ d = \sqrt[3]{LWT} \\ S_P = \dfrac{d}{L} \times 100\% \end{cases} \quad (1)$$

where: V - volume of tiger nuts, cm^3; L - length of tiger nuts, mm; W - width of tiger nuts, mm; T - thickness of tiger nuts, mm; d - equivalent particle size of tiger nuts, mm; S_p - sphericity of tiger nuts, %.

Table 3

Basic physical parameters of tiger nuts

Parametric	Maximum value	Minimum value	Average value	Standard deviation
Volumetric/(cm^3)	2.64	0.62	1.54	0.12
Equivalent particle size/(mm)	13.83	8.54	11.15	0.71
Sphericity/(%)	91	81	85	0.97
Particle density/(kg m^3)	1063.03	1060.46	1062.22	0.78
Kernel mass/(g)	791.20	787.99	789.32	0.52

Elastic Modulus

The elastic modulus, critical for simulation studies, was assessed using the RGM - 4002 universal testing machine (*Sun et al., 2017*), as shown in Fig. 4. Twenty seeds underwent compression testing along the seed thickness axis (*Chen et al., 2023*). The compression test was conducted on the seed along its thickness direction. The speeds were maintained at 2 mm/s before loading, reduced to 0.02 mm/s during loading, and then restored to 2 mm/s after loading. The elastic modulus is calculated as:

$$E = \frac{\sigma}{\upsilon} = \frac{Fl_o}{\Delta l S_o} \tag{2}$$

where: E - elastic modulus of tiger nuts, MPa; σ - compressive stress of tiger nuts, Pa; υ - compressive strain of tiger nuts, Pa; F - exert external force of tiger nuts, N; l_o - initial compression direction length of tiger nuts, mm; Δl - length distortion distance of tiger nuts, mm; S_o - initial cross-sectional area of tiger nuts, mm^2.

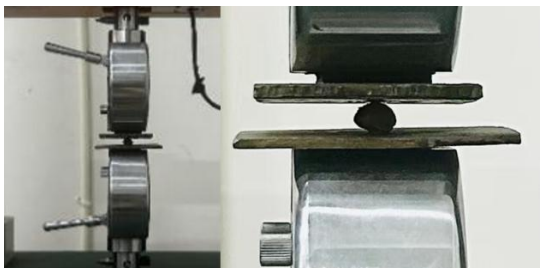

Fig. 4 - Seed compression test of tiger nuts

The experiment was replicated 10 times and the elastic modulus of the tiger nuts was 8.22×106Pa.

Table 4

Elastic modulus of tiger nuts

Parametric	Maximum value	Minimum value	Average value	Standard deviation
Elastic modulus/Pa	9.68×106	6.37×106	8.22×106	0.97

Poisson's ratio and shear modulus

For this experiment, 10 tiger nuts were randomly selected and subjected to a mechanical test using the RGM - 4002 universal testing machine. The seeds were loaded gradually at a speed of 0.2 mm/s in the length direction. Loading was halted when the display indicated that seeds had reached their rupture breakpoints. Simultaneously, a camera mounted parallel to the seed loading platform captured the deformation. The deformations were analyzed using MATLAB, in a manner consistent with the three-axis dimensional measurements, to record the deformation in both the length and the thickness directions (*Khodabakhshian, 2012*). Poisson's ratio was calculated as follows:

$$\delta = \left| \frac{\Upsilon_1}{\Upsilon_2} \right| = \frac{\Delta l / l}{\Delta t / t} \tag{3}$$

where: δ - Poisson's ratio; γ_1 - lengthwise strain of tiger nuts, mm; γ_2 - thickness direction strain of tiger nuts, mm; Δl - longitudinal deformation value of tiger nuts, mm; l - original dimensions in length direction of tiger nuts, mm; Δt - deformation values in the thickness direction of tiger nuts, mm; T - original dimensions in thickness direction of tiger nuts, mm.

Subsequent analysis revealed the shear modulus of the tiger nuts can be obtained. The shear modulus was derived as:

$$G = \frac{E}{2(1+\delta)} \tag{4}$$

where:

G - shear modulus of tiger nuts, Pa; E - elastic modulus of tiger nuts, Pa;

δ - Poisson's ratio of tiger nuts.

As shown in Table 5, the experiment was repeated 10 times and the mean values of Poisson's ratio and shear modulus of tiger nuts were taken as 0.39 and 3.03×106Pa, respectively.

Table 5

Poisson's ratio and elastic modulus of tiger nuts

Parametric	Maximum value	Minimum value	Average value	Standard deviation
Poisson's ratio	0.51	0.28	0.39	0.94
Elastic modulus/P_a	3.58×106	1.97×106	3.03×106	1.10

Friction factor and coefficient of restitution

The determination of the static coefficient of friction between the tiger nuts and various materials - namely the steel plate, acrylic plate, PE polyethylene, and hard plastic plate - was conducted using the oblique measurement method. The experimental setup is depicted in Fig. 5. The seed was placed on the selected material plate, and the handle was rotated to slowly raise the plate. When the seed was about to roll but did not, the rotation of the handle was stopped. The angle between the material plate and the plane α was recorded. The static coefficient of friction was calculated as follows:

$$k = \tan\alpha \tag{5}$$

where: k - static friction factor of tiger nuts; α - angle between the material plate and the plane, °.

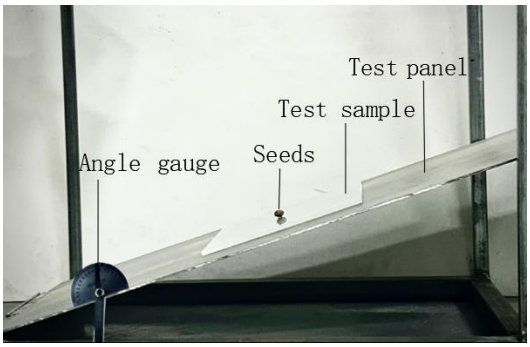

Fig. 5 - Static friction test of tiger nuts

Static friction between the tiger nuts is essential for the accuracy of EDEM simulations. As illustrated in Fig 6, A4 paper was employed as the sample plate, to which double-sided adhesive tape was applied. Randomly selected tiger nuts of comparable size were randomly distributed on the sample plate, which was subsequently positioned on the test bench. The handle was rotated until the seeds demonstrated a tendency to roll downwards without actual rolling. At this juncture, the rotation of the handle was stopped. The angle between the seed plate and the plane was recorded α, which could be substituted into the aforementioned equation (*Wu et al., 2020; Shi et al 2019*). The static friction between the seeds can be obtained by substituting into the above equation. The tests involving tiger nuts and various materials were repeated 20 times. The results are shown in Table 6. The resultant mean static friction values for tiger nuts in contact with steel, acrylic, plastic and seed plates were 0.40, 0.41, 0.57 and 0.49 respectively.

Table 6

Static friction factor of tiger nuts

Parametric	Maximum value	Minimum value	Average value	Standard deviation
tiger nuts - steel plate	0.43	0.37	0.40	0.45
tiger nuts - acrylic sheet	0.49	0.23	0.41	0.51
tiger nuts - plastic sheet	0.63	0.51	0.57	0.49
tiger nuts - seed board	0.58	0.36	0.49	0.53

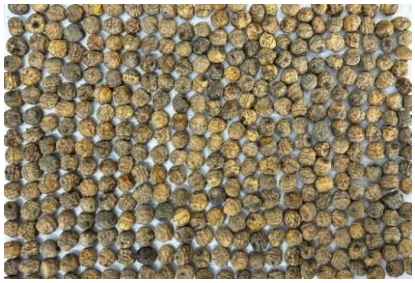

Fig. 6 - Tiger nuts board

Determination of rolling friction factor of tiger nuts

The rolling friction factor of tiger nuts correlates with their size, volume and sphericity. In this study, 10 tiger nuts with a high degree of sphericity were assessed using the oblique measurement method. Steel, acrylic, plastic and seed boards were selected for the test. On the test bench, different test plates were positioned, and the seed was placed on the material plate. The handle was then turned to gradually increase the angle between the experimental plate and the horizontal plane. The adjustment was halted when the seeds appeared to roll, and the angle of the inclined plane at this time was recorded as β. This angle was then substituted into equation 5 to calculate the rolling friction factor.

The above tests were replicated 20 times for each group, as shown in Table 7, with the mean rolling friction factors being 0.24, 0.21, 0.17, and 0.27 for steel, acrylic, plastic and seed plates, respectively.

Table 7

Rolling friction factor of tiger nuts

Parametric	Maximum value	Minimum value	Average value	Standard deviation
Tiger nuts - steel plate	0.31	0.17	0.24	0.63
Tiger nuts - acrylic sheet	0.25	0.16	0.21	0.56
Tiger nuts - plastic sheet	0.24	0.11	0.17	0.55
Tiger nuts - seed board	0.33	0.19	0.27	0.59

Coefficient of restitution for tiger nuts

The coefficient of restitution was defined as the ratio of the relative normal separation velocity post-collision to that prior to collision (i.e., the ratio of the maximum height of rebound of the tiger nuts after collision with an object to the initial height of fall). The coefficient of restitution significantly influences the realism of EDEM simulation metrics (*Yu et al., 2020*). In this study, the seeds were allowed to freely fall and collide with a plate, with their trajectories subsequently recorded. Before the test, coordinate-scale paper was placed at 90° to the material plate, forming a two-dimensional spatial coordinate system. Seeds were released from a height of 250 mm above the plate. An iPhone 14 was employed to capture the rebound at a slow-motion frame rate of 120fps, as depicted in Fig. 7, thereby facilitating accurate rebound height measurements. The coefficient of restitution equation is:

$$e = \left|\frac{v'}{v}\right| = \left|\frac{v_2' - v_1'}{v_1 - v_2}\right| = \left|\frac{-\sqrt{2gh'}}{\sqrt{2gh}}\right| = \sqrt{\frac{h'}{h}} \tag{6}$$

where: e - coefficient of restitution of tiger nuts; $v`$ - instantaneous velocity of tiger nuts in the normal direction before collision, mm/s; $v$ - instantaneous velocity of tiger nuts before collision, mm/s; $v_1`$ - velocity of tiger nuts before collision, mm/s; $v_2`$ - velocity of material before collision, mm/s; $v_1$ - velocity of tiger nuts after collision, mm/s; $v_2$ - velocity of material after collision, mm/s; $g$ - gravitational acceleration; $h$ - initial drop height of tiger nuts, mm; $h`$ - maximum rebound height of tiger nuts after collision, mm.

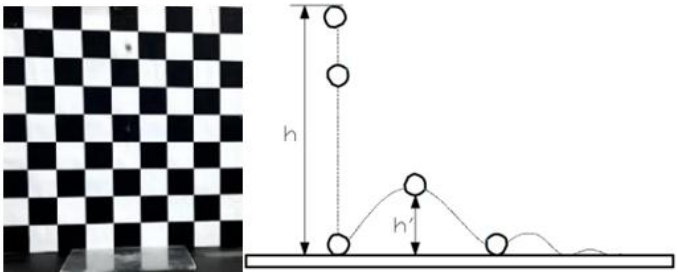

Fig. 7 - Seed coefficient of restitution tests of tiger nuts

Observations indicate that when the rebound effect is not the desired effect, it notably affects the coefficient of restitution test. Given the irregular geometry of the tiger nuts, it is difficult for them to rebound vertically upwards after hitting a flat plate. Consequently, extensive testing is required to investigate this phenomenon.

The results of 20 tests in which the rebound path was parallel to the fall path are selected for analysis. The average value from these tests was used in the above formula for calculation. As shown in Table 8, the mean coefficients of restitution for collisions between tiger nuts and various materials — steel plate, acrylic plate, plastic plate, and seed plate — were 0.63, 0.58, 0.55, and 0.53, respectively, with corresponding standard deviations of 0.61, 0.56, 0.63, and 0.58.

Table 8

Coefficient of restitution of tiger nuts

Parametric	Maximum value	Minimum value	Average value	Standard deviation
Tiger nuts - steel plate	0.81	0.47	0.63	0.61
Tiger nuts -acrylic sheet	0.78	0.37	0.58	0.56
Tiger nuts - plastic sheet	0.76	0.34	0.55	0.63
Tiger nuts - seed board	0.77	0.28	0.53	0.58

Physical stacking angle tests

The stacking angle embodies the comprehensive performance of seeds, including inter-crop mobility and crop-material mobility, as well as inter-crop friction and crop-material friction properties (*Xia et al., 2019; Hamzah et al., 2018; Ma et al., 2020*), which are pivotal for achieving accurate results in EDEM simulations. The parameters for a single seed model, particularly for diverse shapes like those of tiger nuts, are not universally applicable. In the present study, physical experiments were integrated with EDEM simulations to calibrate the parameters of the seed stacking angle of tiger nuts for the above characteristics.

The determination of the stacking angle was performed using the draw plate method (*Yu et al., 2021*). The testing apparatus comprised a stainless steel cylindrical drum, 130 mm in outer diameter, 125 mm in inner diameter, and 150 mm in height, without a lid. This drum was positioned on a flat test bed and filled to the brim with tiger nuts. As the cylinder was gradually raised, the seed freely formed a conical shape, and the angle of the resultant seed slope was recorded as the stacking angle when no further seed flow was observed, as shown in Fig. 8 (a).

In this study, the stacking angle was documented utilizing a MATLAB image processing technique (*Müller et al., 2021*). As illustrated in Fig. 8 (a), the image was captured using the imread function, Fig. 8 (b) shows the image grayscale, and as shown in Fig. 8 (c), the grayscale image was binarized using the im2bw function by selecting the appropriate threshold. As shown in Fig. 8 (d), the image, characterized by large internal gaps and incoherent structures at the edges, was refined using the imfill function to improve the definition of structural elements. The binarized contours were extracted with the bwperim function, as indicated in Fig. 8 (e). Half of the edge information was imported into Origin and analyzed using the image digitization tool to determine the tangent, as shown in Fig. 9.

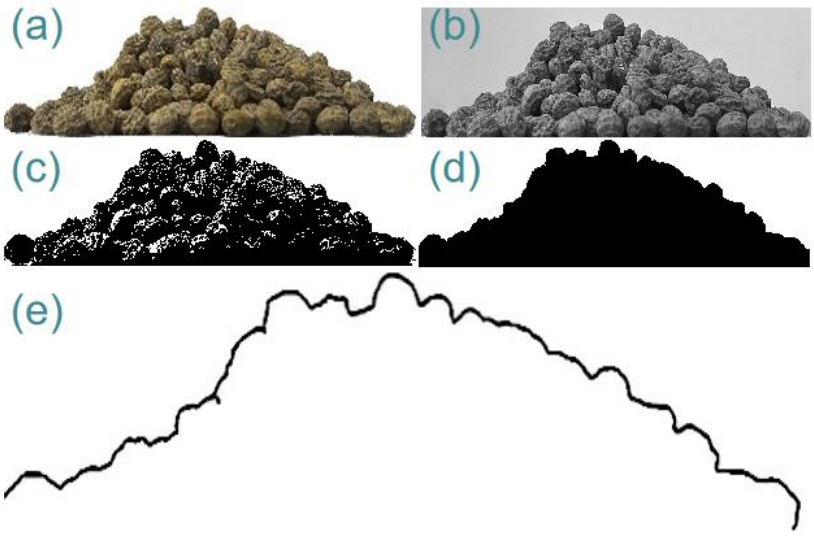

Fig. 8 - Stacked corner contour extraction process

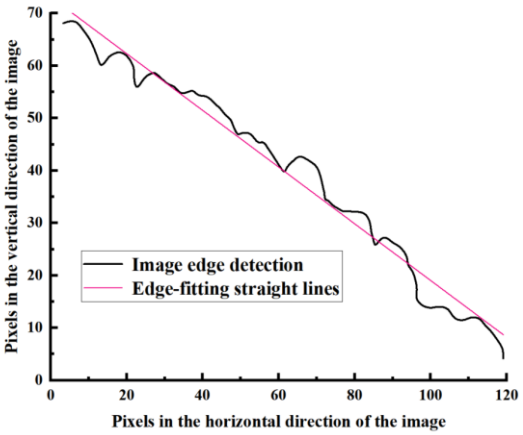

Fig. 9 - Tangent value fit

The experiment was replicated across 10 groups, and the results of the physical slope tangent τ measurements of seed stacking angle are presented in Table 9, with an average value of 0.734 recorded.

Table 9

Measurements of the angle of accumulation of tiger nuts

Test number	1	2	3	4	5	6	7	8	9	10
Stacking angle tangent	0.71	0.74	0.73	0.71	0.69	0.74	0.77	0.75	0.74	0.76

Stacking angle simulation test

From the data of 200 measurements, most of the tiger nuts were predominantly of an oblate-spheroid shape, with variations within 3 mm in thickness. A seed model was constructed using SolidWorks, as illustrated in Fig. 10 (b). Considering the variability in seed sizes, 50 percent of the seeds were model at dimensions of 13.5 mm in height, 12 mm in width, and 8.15 mm in thickness, while 25 percent of the seeds were scaled down by a factor of 0.9 and 0.8 respectively. The model was converted to STL format and imported into EDEM, filled with particles no smaller than 1 mm with the smoothing value set to 1, culminating in 245 different particles, as shown in Fig. 10 (c).

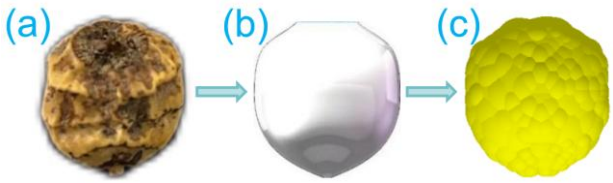

Fig. 10 - Seed model building process

To ensure consistency between the simulation process and the physical experiment, the material dimensions used in the simulation are identical to those used in the physical experiment in SOLIDWORKS, the material properties selected in EDEM are the same as the actual situation, and the input parameters are consistent with the measured data. The different materials are shown in Table 10. In this study, 500 particles were selected for generation and subsequently deposited for a duration of 1.5 s. The cylindrical container was elevated vertically at a velocity of 0.03 m/s, facilitating the autonomous flow of seeds, thereby forming a stacking angle. The total simulation was conducted over a period of 6 s. The simulation outcomes were documented upon completion. The results of the test are shown in Fig. 11. The resultant images were processed in MATLAB and analyzed using the image digitization tool to derive the tangent values in Fig. 12.

Table 10

Contact material simulation parameters

Parametric	Average parameters of steel plates	Average parameters of plastic plates
Poisson's ratio	0.30	0.34
Density/kg m^{-3}	7800	1160
shear modulus/MPa	79100	9420

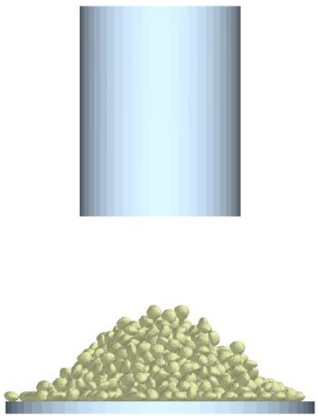

Fig. 11 - Simulation results before parameter optimization

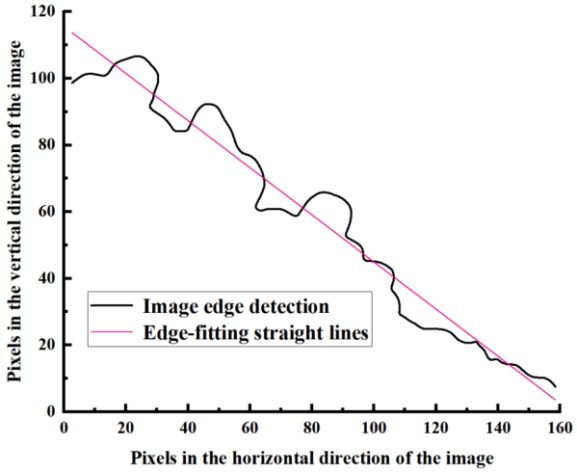

Fig. 12 - Simulation of the fitted image

Parameter optimization for discrete element simulation

Plackett-Burman design was employed for the screening test, utilizing Design-Expert 13 software. This design encompassed a multi-parametric experiment with two levels, nine principal factors, and two dummy factors to assess interactions between tiger nuts and various materials. The main effects of the factors were estimated using the minimum number of trials required to identify those with significant influence on the indicators being examined (*Yuan et al., 2022; Liu et al., 2016*).

Determination of significant impact parameters

X_1~X_8 represent the primary characteristics of tiger nuts, while X_9~X_{11} denote horizontally replicated tests. The maximum and minimum settings of the 12 test parameters were coded as +1 and -1, based on literature review and empirical data (e.g., Table 11) for each of the 12 sets of tests. Using the stacking angle as the principal factor under investigation, the images obtained from each group of tests were analyzed using MATLAB and the image digitization tool to record the values, as shown in Table 12.

Table 11

Plackett-Burman Test Parameter Range Tables

Symbols	Test parameters	Low level (-1)	Hight level (+1)
X_1	Poisson's ratio of tiger nuts	0.25	0.45
X_2	tiger nuts shear modulus/MPa	25.9	35.9
X_3	Tiger nuts - tiger nuts rolling friction coefficient	0.21	0.31
X_4	Tiger nuts - tiger nuts coefficient of static friction	0.28	0.68
X_5	Tiger nuts - tiger nuts coefficient of restitution	0.28	0.78
X_6	Tiger nuts - acrylics plate coefficient of restitution	0.37	0.78
X_7	Tiger nuts - acrylics plate static friction coefficient	0.23	0.49
X_8	Tiger nuts - acrylics plate rolling friction coefficient	0.17	0.23
$X_{9,\ 10,\ 11}$	Tiger nuts -nylon Horizontal repetition test	—	—

Table 12

Plackett-Burman test program and results

No.	X_1	X_2	X_3	X_4	X_5	X_6/X_9	X_7/X_{10}	X_8/X_{11}	Stacking angle tangent
1	1	1	-1	1	1	1/-1	-1/1	-1/-1	0.72
2	-1	1	1	-1	1	1/-1	1/-1	-1/1	0.87
3	1	-1	1	1	-1	1/-1	1/-1	1/-1	1.21
4	-1	1	-1	1	1	-1/1	1/-1	1/-1	0.71
5	-1	-1	1	-1	1	1/1	-1/1	1/-1	0.96
6	-1	-1	-1	1	-1	1/1	1/1	-1/1	0.76
7	1	-1	-1	-1	1	-1/-1	1/1	1/1	0.69
8	1	1	-1	-1	-1	1/1	-1/-1	1/1	0.73
9	1	1	1	-1	-1	-1/1	1/1	-1/-1	0.79
10	-1	1	1	1	-1	-1/-1	-1/1	1/1	1.09
11	1	-1	1	1	1	-1/1	-1/-1	-1/1	1.10
12	-1	-1	-1	-1	-1	-1/-1	-1/-1	-1/-1	0.71

Analysis of the results indicates that when the P-value is greater than 0.05, it signifies an absence of significant influence on the stacking angle, whereas a P-value less than 0.05 denotes a substantial influence on the stacking angle. As illustrated in Table 13, the P-values for X_1, X_2, X_5~ X_8 exceeded 0.05, with corresponding effects on the stacking angle of 0.36%, 5.66%, 1.33%, 0.75%, 1.90% and 4.16%, respectively. The influence of X_3 and X_4 accounted for 64.89 percent and 16.08 percent, respectively. Compared with other individual factors, X_3 and X_4 emerged as the predominant influences, collectively accounting for 80.97 percent of the influence factors, thereby confirming them as the main influence factors. By comparing the values, the primary and secondary order of parameter is: X_3, X_4, X_2, X_8, X_7, X_5, X_6, X_1.

Table 13

Significance analysis of Plackett-Burman test parameters

Parameters	Standardization effect	Sum of squares	Contribution rate/%	F value	P value
model		0.35		8.91	0.04
X_1	0.21	0.01	0.36	0.27	0.64
X_2	-0.08	0.02	5.66	4.24	0.13
X_3	0.28	0.24	64.89	48.61	0.01
X_4	0.14	0.06	16.08	12.05	0.04
X_5	-0.04	0.01	1.33	1.00	0.39
X_6	0.03	0.01	0.75	0.56	0.51
X_7	-0.05	0.01	1.90	1.42	0.32
X_8	0.07	0.02	4.16	3.11	0.18

*Note: * indicates a significant impact (0.01<P<0.05) ; ** indicates that the effect is extremely significant (P≤0.01).*

Steepest climb test based on the Plackett-Burman test

It was determined from the significance influence parameter test that X_3 and X_4 exerted the most substantial impact on the stacking angle; hence, they were selected as the test factors in the steepest climb test. The remaining parameters were modeled based on the values derived from the physical experiment results. X_3, X_4 showed that the standardized effect was positive, so it was incrementally increased at a fixed step size during the steepest climb test. The relative error 3 was calculated by bringing the steepest climb test stack angle tangent θ and the physical test stack angle tangent τ into Eq. 7.

The results of the steepest climb test are shown in Table 14, in which the rolling friction coefficients and static friction coefficients between the seeds were taken as 0.21~0.31 and 0.28~0.68, respectively, and the relative error of test 2 of the test results was the smallest, so test 2 was chosen as the center of the subsequent center-conformity response surface test. The optimal intervals are the values in the vicinity where the error is minimized: test 1 and test 3, the low and high values, respectively.

$$\ell = \frac{|\tau - \theta|}{\tau} \times 100\% \quad (7)$$

Table 14

Steepest Climb Test Program and Results

No.	X_3	X_4	Climbing test stacking angle tangent	Relative error/%
1	0.21	0.28	0.72	2.09
2	0.24	0.38	0.76	1.48
3	0.26	0.48	0.78	5.41
4	0.29	0.58	0.80	8.37
5	0.31	0.68	0.82	10.27

RESULTS AND DISCUSSION

Analysis of simulation results

Based on the range of interval values of rolling and static friction factors selected for tiger nuts in the steepest climb test using Design-Expert 13, the central composite test was conducted in Design-Expert 13. Stacking angle tests were performed for 11 sets of parameters. In order to increase the precision and reliability of the test and to reduce the effect of random errors on the test results, three of the groups of parameters were horizontally repeated tests. This was done to assess the impact of the rolling friction factor X_3 and static friction factor X_4 on the response surface optimization test for the formation of stacking angle of tiger nuts. The coding of the test factors and the results are displayed in Table 15. The maximum error in this test result was 4.84%, which is a substantial reduction of 5.43% relative to the maximum error of 10.27% for the steepest climb test. The minimum error of 0.12% is 1.35% less than the minimum error of 1.47% for the steepest climb test. The results show a substantial increase in the accuracy and reliability of the results obtained in this interval.

Table 15

Centre composite test results

No.	X_3	X_4	Stacking angle tangent	Errors/%
1	-1	-1	0.75	2.54
2	1	-1	0.73	0.55
3	-1	1	0.75	3.19
4	1	1	0.76	4.84
5	-1.41	0	0.75	2.80
6	1.41	0	0.75	2.54
7	0	-1.41	0.74	0.12
8	0	1.41	0.76	4.59
9	0	0	0.74	1.49
10	0	0	0.74	1.36
11	0	0	0.74	1.49

Multiple regression fitting by Design-Expert 13-centre composite test yielded the second-order regression equations for the coefficients of rolling and static friction between the simulation test stacking angle and the tiger nuts as:

$$\theta = 0.918 + 0.0844\,X_3 + 0.0284\,X_4 - 0.0785\,X_3X_4 - 0.0575\,X_3^2 - 0.084X_4^2 \quad (8)$$

As can be seen from Table 16, the P-value for the tiger nuts model is less than 0.0001. The misfit direction P is 0.8422, and the coefficient of determination R^2 is 0.9992, which is close to 1, indicating an extremely significant regression equation. A comparison between the adjusted coefficient of determination Adjusted R^2 and Predicted R^2 is 0.013, which is less than 0.2. The coefficient of variation (CV) is relatively small at 5.8%, which indicates a higher reliability of the model, as evidenced by these experimental results. It is concluded that the regression model not only accurately captures the real situation but also effectively predicts the stacking angle of tiger nuts.

Table 16

Analysis of variance results of the central composite response surface regression model

Parameters	Sum of squares	Degrees of freedom	Mean square	F value	P value
model	0.0011	5	0.0002	1204.94	＜0.0001
X_3	0.000003	1	0.000002	15.47	0.0110
X_4	0.0007	1	0.00007	3710.36	＜0.0001

Parameters	Sum of squares	Degrees of freedom	Mean square	F value	P value
X_3X_4	0.0002	1	0.0002	1040.67	＜0.0001
X_3^2	0.0001	1	0.0001	652.97	＜0.0001
X_4^2	0.0002	1	0.0002	962.79	＜0.0001
residual	0.0000009	5	0.0000002	/	/
lost proposal	0.0000003	3	0.0000001	0.2750	0.8422
pure error	0.0011	2	0.0000003	/	/

*Note: * indicates a significant impact (0.01<P<0.05) ; ** indicates that the effect is extremely significant (P≤0.01).*

The stacking angle response surface is depicted in Fig. 13, where variations in the effect on the stacking angle are associated with changes in dynamic and static friction. The coefficient of rolling friction has a small interval of variation, whereas an increase in the coefficient of static friction correlates with an increase in the stacking angle. The most pronounced impact on the stacking angle occurs when the rolling friction coefficient is 0.21 and the static friction coefficient is 0.48. When the rolling friction coefficient is between 0.23~0.26, the model shows a slowly increasing trend. When the static friction of the seeds increases, the effect on their stacking angle is greater regardless of whether the rolling friction is smaller or greater. This indicates that the coefficient of static friction has a greater effect on the change in the value of the tiger nuts stacking angle compared to the coefficient of dynamic friction. Combined with the previous analyses in this paper, the significance of the influence of static friction and rolling friction on the stacking angle between the tiger nuts were better verified.

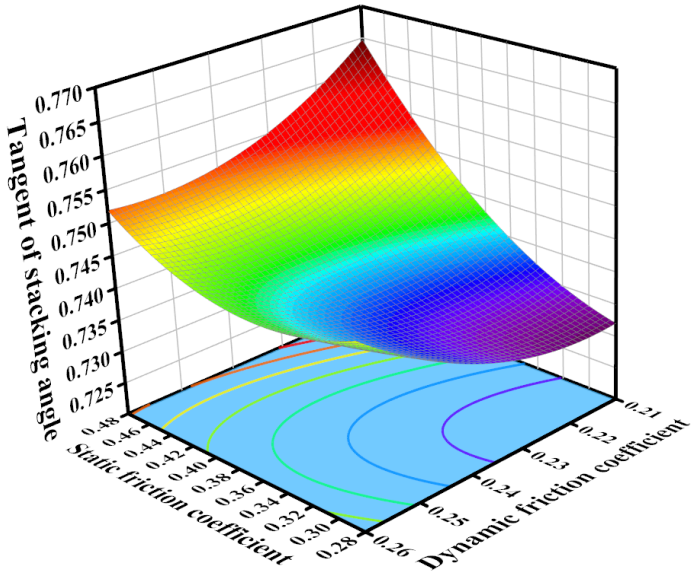

Fig. 13 - Stacking angle response surface plot

Experimental verification

In order to make the simulated stacking angle close to the physical experiment, this analysis is based on the central composite test and the second-order regression equation. From the objective of minimizing the error of the test results, the optimal solution analysis is carried out for the rolling friction and static friction between the seeds, which have the most influence in the test. The objective function and constraints are set as follows:

$$\begin{cases} \min \omega(X_3, X_4) \\ s.t. \begin{cases} 0.21 \le X_3 \le 0.26 \\ 0.28 \le X_4 \le 0.48 \end{cases} \end{cases} \quad (9)$$

The optimal parameters for static and rolling friction between tiger nuts were identified as 0.32 and 0.24, respectively. The stacking angle of the simulation test is closest to the stacking angle of the physical test, indicating that this combination is the best parameter combination to be used in the simulation test.

To confirm the reliability of the parameter results, the optimal parameters were applied to simulation tests in EDEM, and the tests were replicated three times, yielding the simulation stacking angle tangent values of 0.720, 0.732, and 0.741, respectively. The error between the simulation test stacking angle mean value of 0.731 and the result from the physical test, recorded at 0.734 is 0.41%. A high degree of congruence is observed between the physical test 14(a) and the simulation of stacking angle 14(b) employing the selected optimal parameters, with no significant difference evident. This suggests that the parameters of this simulation test are set with precision. This result further validates the reliability and realism of the simulation test.

Compared with existing studies, this paper improves the accuracy of the model through a combination of physical and simulation tests. The obtained parameters can be directly used in the testing of tiger nutsing tools and provide a reliable discrete element parameter model.

Fig. 14 - Simulation of stacking angle after parameter optimization of tiger nuts

CONCLUSIONS

In this study, MATLAB was used to make accurate and fast measurements of the three dimensions of tiger nuts to obtain reliable discrete meta-model dimensions. The average density and thousand grain weight of tiger nuts were measured to be 1062.22 kg/m^3 and 789.32 g, respectively. The average volume, equivalent particle diameter and sphericity were 1.54 cm^3, 11.15 mm and 85%, respectively. The modulus of elasticity, Poisson's ratio and shear modulus of tiger nuts were measured in physical tests: 8.22×106 Pa, 0.39, 3.03×106 Pa.

Dimensional measurements and physical tests of tiger nuts were used as a basis for selecting parameters for simulation tests. Through the Plackett-Berman screening experiment and the steepest-climbing test, the parameter intervals that had a large influence on the stacking angle were identified: inter-seed rolling friction (0.21 to 0.31), and inter-seed static friction (0.28 to 0.68). The optimal simulation parameters were obtained from the central composite response surface test: inter-seed rolling friction of 0.24 and inter-seed static friction of 0.32, the relative error in the stacking angle was minimized.

In this paper, the relevant parameters obtained from the discrete element calibration test using tiger nuts can be used as the parameters for tiger nuts simulation, and can be used as a reference for the optimized design of tiger nuts sowing machine structure. By simulating the process of stacking angle formation of tiger nuts, it is possible to predict the pass rate and breakage rate of sown seeds under different factors. This optimizes the structure of the tiger nuts planter, reduces the number of physical pre-tests, avoids the problem of not being able to conduct seeding tests due to external environmental factors, reduces production costs, and improves research efficiency.

ACKNOWLEDGEMENT

The authors were funded for this project by the Ministry of Agriculture and Rural Affairs Specialty Oilseed (Oil Sesame) Crop Full Mechanization Base, and the Key R&D Tasks in the Autonomous Region (2023B02032).

REFERENCES

[1] Chen X., Zhong L. (2012). Design and testing of air-absorbent seed dischargers with seed guides (气吸式排种器带式导种装置的设计与试验). *Journal of Agricultural Engineering*, Vol. 28(22), pp. 8-15, China.

[2] Chen Y., Gao X., Jin X., Ma X., Hu B., Zhang X. (2023). Calibration and test of discrete element simulation parameters for tiger nut seeds (油莎豆排种离散元仿真参数标定与试验). *Journal of Agricultural Machinery*, Vol. 54(12), pp. 58-69, China.

[3] Chen Y., Wang K., Luo X., Li J., Hu B., Zhang H. (2017). Theoretical analysis of adsorption seed pick-up in air-blown suspended seed supply drum planters (气吹悬浮供种滚筒式播种机吸附取种理论分析). *Agricultural mechanization research*, Vol. 39(04), pp. 21-26, China. DOI: 10.13427/j.cnki.njyi.2017.04.004.

[4] Guo T., Wan C., Huang F., Wei C., Hu Z. (2021). Progress of research on the main nutrients and physiological functions of tiger nut seeds (油莎豆主要营养成分及生理功能研究进展). *Chinese Journal of Oil Crops*, Vol. 43(06), pp. 1007-9084, China DOI: 10.19802/j.issn.1007-9084.2020145.

[5] Hamzah M., Beakawi A, H., Omar S. (2018). A review on the angle of repose of granular materials. *Powder Technology*, Vol. 330(03), pp. 397-417.

[6] Hou Z., Dai N., Chen Z., Xu Y., Zhang X. (2020). Determination of physical property parameters of iceplant seeds and calibration of parameters for discrete element simulation (冰草种子物性参数测定与离散元仿真参数标定). *Journal of Agricultural Engineering*, Vol. 36(04), pp. 44-53, China.

[7] Hu M., Xia J., Zhou Y., Luo C., Zhou M., Liu Z. (2022). Measurement and Calibration of the Discrete Element Parameters of Coated Delinted Cotton Seeds (涂层脱绒棉籽离散元素参数的测量与校准). *Agriculture*, Vol. 12, 286, China. https://doi.org/10.3390/agriculture12020286

[8] Khodabakhshian R. (2012). Poisson's ratio of pumpkin seeds and their kernels as a function of variety, size, moisture content and loading rate. Agricultural Engineering International: *The CIGR e-journal*, Vol. 14(3), pp. 3-14.

[9] Li Z., Wang J., Liu H., Wang P., Wu X., Ma C., Zhang D. (2022). Status of tiger nut seeds Industry Development and Suggestions (油莎豆产业发展现状及建议). *Modern agricultural science and technology*, Vol. 22(08), pp. 225-231, China.

[10] Liu F., Zhang J., Li B., Chen J. (2016). Discrete elemental parameter analysis and calibration of wheat based on stacking tests (基于堆积试验的小麦离散元素参数分析及标定). *Journal of Agricultural Engineering*, Vol. 32(12), pp. 247-253, China.

[11] Ma Y. (2015). *Agricultural material science (农业材料科学).* Beijing: Chemical Industry Press, 2015, China.

[12] Ma Y., Song C., Xuan C., Wang H., Yang S., Wu P. (2020). Calibration of discrete element model parameters for alfalfa straw compression simulation (苜蓿秸秆压缩仿真离散元模型参数标定). *Journal of Agricultural Engineering*, Vol. 36(11), pp. 22-30, China.

[13] Muller D., Fimbinger E., Brand C. (2021). Algorithm for the determination of the angle of repose in bulk material analysis. *Powder Technology*, Vol. 383(01), pp. 598-605. https://doi.org/10.1016/j.powtec.2021.01.010

[14] Peng F., Wang J., Zhang L., Wei C., Liu W. (2022). Improvement and parameter optimisation of air suction cup seed discharger for tiger nut seeds (油莎豆气吸盘式排种器改进和参数优化). *Agricultural Engineering*, Vol. 12(12), pp. 98-103, China. DOI: 10.19998/j.cnki.2095-1795.2022.12.017.

[15] Shi L., Ma Z., Zhao W., Yang X., Sun B., Zhang J. (2019). Calibration of discrete meta-simulation parameters and experimental validation of seed rowing in caraway seeds (胡麻籽粒离散元仿真参数标定与排种试验验证). *Journal of Agricultural Engineering*, Vol. 35(20), pp. 25-33, China.

[16] Sun J., Yang Z., Guo Y., Cui Q., Wu X., Zhang Y. (2017). Mechanical properties of compression and damage crack formation mechanism in cereal grains (谷子籽粒压缩力学性质及损伤裂纹形成机理). *Journal of Agricultural Engineering*, Vol. 33(18), pp. 306-314, China.

[17] Tsa B., Rf B., Er B. (2021). Classification of granular materials via flowability-based clustering with application to bulk feeding. *Powder Technology*, Vol. 378(02), pp. 288-302. https://doi.org/10.1016/j.powtec.2020.09.022

[18] Wang L., He X., Hu C., Guo W., Wang X., Xing J., Hou S. (2022). Determination of physical property parameters of dressed cotton seeds and calibration of parameters for discrete element simulation (包衣棉种物性参数测定与离散元仿真参数标定). *Journal of China Agricultural University*, Vol. 27(06), pp. 71-82, China.

[19] Wu M., Cong J., Yan Q., Zhu T., Peng X., Wang Y. (2020). Calibration and experimentation of parameters for discrete meta-simulation of peanut seed particles (花生种子颗粒离散元仿真参数标定与试验). *Journal of Agricultural Engineering*, Vol. 36(23), pp. 30-38, China.

[20] Xia R., Li B., Wang X., Li T., Yang Z. (2019). Measurement and calibration of the discrete element parameters of wet bulk coal (湿煤颗粒离散元素参数的测量与校准). *ScienceDirect. Measurement*, Vol. 142(2019), pp. 84-95, China. https://doi.org/10.1016/j.measurement.2019.04.069

[21] Xu Z., Zhou Y., Hu M., Ke H., Zhang M., Lv W. (2020). Simulation test on seed discharge of internal seed filling type cotton seed discharger based on EDEM (基于 EDEM 的内充种式棉花排种器排种仿真试验). *Journal of Gansu Agricultural University*, Vol. 55(04), pp. 175-183, China. DOI: 10.13432/j.cnki.jgsau.2020.04.025.

[22] Yu C., Duan H., Cai X., Xu T., Yao F., Chen Z., Yan Q. (2021). Determination of micro potato materials based on discrete element simulation parameters (基于离散元仿真参数的微型薯物料测定). *Journal of Central China Agricultural University*, Vol. 40(01), pp. 210-217, China. DOI: 10.13300/j.cnki.hnlkxb.2021.01.026.

[23] Yu Q., Liu Y., Chen X. (2020). Calibration and testing of simulation parameters of Panax pseudoginseng seeds based on discrete elements (基于离散元的三七种子仿真参数标定与试验). *Journal of Agricultural Machinery*, Vol. 51(02), pp. 123-132, China.

[24] Yuan J., Zhang H., Yang S., Song Q., Zhang J. (2022). Discrete meta-parameter calibration of grass carp feeds based on stacking tests (基于堆叠试验的草鱼饲料离散元参数校准). *Manufacturing automation*, Vol 44(12), pp. 61-67, China.

[25] Zeng Z., Ma X., Cao X., Li Z., Wang X. (2021). Current status and perspectives of the application of the discrete element method in agricultural engineering research (离散元法在农业工程研究中的应用现状和展望). *Journal of Agricultural Machinery*, Vol. 52(04), pp. 1-20, China.

[26] Zhang S., Zhang R., Chen T., Fu J., Yuan H. (2022). Mung bean seed discrete meta-simulation parameter calibration and seed scheduling test (绿豆种子离散元仿真参数标定与排种试验). *Journal of Agricultural Machinery*, Vol. 53(03), pp. 71-79, China.

[27] Zhang X., Chen Y., Shi Z., Jin W., Zhang H., Fu H., Wang D. (2021). Design and experiment of double-storage turntable cotton vertical disc hole seeding and metering device (双仓转盘式棉花竖直圆盘穴播排种器设计与试验). *Transactions of the Chinese Society of Agricultural Engineering*, Vol. 37(19), pp. 27-36, China.

[28] Zhang X., Cheng J., Shi Z., Wang M., Fu H., Wu H. (2023). Simulation and experiment of seed taking performance of swing clamp type maize precision seed-metering device (摆动夹取式玉米精量排种器取种性能仿真与试验). *Transactions of the Chinese Society of Agricultural Machinery*, Vol. 54(04), pp. 38-50, China.

[29] Zheng X., He X., Shang S., Wang D., Li C., Shi Y., Zhao Z., Lu Y. (2024). Calibration and test of discrete element simulation parameters for tiger nut seeds grain (油莎豆种子籽粒离散元仿真参数标定与试 验). *Agricultural Mechanisation Research*, Vol. 46(2), pp. 172-178, China. DOI:10.13427/j.cnki.njyi.2024.02.028.

[30] Zhou H., Hu Z., Chen J., Lv X., Xie N. (2018). Calibration of DEM models for irregular particles based on experimental Check for design method and bulk experiments (基于实验数据校准不规则颗粒的数字高程模型（DEM）验证设计方法和体积试验). *Powder Technology*, Vol. 33(02), pp. 210-223, China. https://doi.org/10.1016/j.powtec.2018.03.064.